ELSEVIER

Polymer 42 (2001) 7203–7208

polymer

www.elsevier.nl/locate/polymer

Polymer Communication

Stress relaxation experiments on a lamellar polystyrene–polyisoprene diblock copolymer melt

Peter Holmqvist[a], Valeria Castelletto[a], Ian W. Hamley[a,*], Nadja Hermsdorf[b], Kristoffer Almdal[b]

[a]*School of Chemistry, University of Leeds, Leeds LS2 9JT, UK*
[b]*Department of Condensed Matter Physics and Chemistry, Risø National Laboratory, DK-4000 Roskilde, Denmark*

Received 14 December 2000; received in revised form 21 February 2001; accepted 23 February 2001

Abstract

The non-linear rheology of the lamellar phase of a polystyrene–polyisoprene diblock copolymer is studied by oscillatory shear experiments. The relaxation of the shear modulus, $G(t, \gamma)$ is studied as a function of strain amplitude, γ, up to large amplitude strains, $\gamma = 100\%$. The decay of $G(t, \gamma)$ is analysed using the model-independent CONTIN inverse Laplace transform algorithm to obtain a series of relaxation times, which reveals multiple relaxation processes. The timescale for the fastest relaxation processes is compared to those previously observed for diblock copolymer melts via dynamic light scattering experiments. The slowest relaxation process may be related to the shear-induced orientation of the lamellae. It is shown that time-strain separability $G(t, \gamma) = G(t)h(\gamma)$ can be applied, and the damping function $h(\gamma)$ is consistent with a strongly strain-softening system exhibiting plastic flow at large strains.

1. Introduction

Block copolymers are a fascinating class of nanostructured soft material [1,2]. Upon lowering temperature from the one phase region, most polymer mixtures undergo phase separation. However, in block copolymers, this energetically favourable macrophase separation is prevented by the connectivity of the blocks, and instead microphase separation occurs. This leads to the formation of a number of ordered morphologies, in which the structural periodicity is typically 10–100 nm. We consider here the simplest type of block copolymer, a symmetric AB diblock. A morphology diagram can be assembled by determining the phases formed as a function of temperature for a diblock with a given composition, f_A (volume fraction of A block). The morphology diagram for a particular diblock system is usually parameterised in terms of f_A and χN. Here χ is the Flory-Huggins interaction parameter and N is the degree of polymerisation. For symmetric diblock copolymers ($f_A = 0.5$) a lamellar phase is stable. For more asymmetric diblocks, bicontinuous cubic gyroid, hexagonal-packed cylinder and body-centered cubic spherical structures have also been identified [1].

The linear viscoelastic response of block copolymers has been extensively exploited to determine order–order and order–disorder phase transitions. When varying temperature, the isochronal dynamic shear moduli exhibit a discontinuity at a phase transition that reflects differences in the low frequency mechanical properties of different structures [3–6].

Despite the extensive use of the linear viscoelastic response to probe block copolymer ordering, we are not aware of any studies that focus on the non-linear rheological behaviour of block copolymer melts, although there has been work on micellar block copolymer solutions [7–10]. Nonetheless, non-linear shear flows are essential in order to macroscopically orient block copolymers by large amplitude oscillatory shear, a process that has been extensively exploited [1,6,11,12]. Non-linear extensional flows are also central to the orientation of block copolymers by extrusion [11,13–15], for example during processing, and the drawing behaviour of block copolymer thermoplastic elastomers has been widely studied.

The purpose of the present work is to investigate for the first time the relaxation processes that occur in a lamellar block copolymer in the non-linear viscoelastic regime. We analyse the modulus obtained from stress relaxation experiments, which indicates multiple relaxation processes. We then discuss possible relationships between the rheological timescales and those obtained from dynamic light scattering

* Corresponding author. Tel.: +44-113-233-6430; fax: +44-113-23-6565.
E-mail address: I.W.hamley@chem.leeds.ac.uk (I.W. Hamley).

0032-3861/01/$ - see front matter
PII: S0032-3861(01)00161-6

experiments on similar diblock copolymer melts. Finally, the form of the damping function for the strongly strain softening system is considered.

2. Experimental

2.1. Characterisation of polymers

The polyisoprene–polystyrene diblock copolymer was synthesised by anionic polymerisation using established procedures [16,17]. The polymerisation was carried out at 313 K using s-butyllithium as the initiator and cyclohexane as the solvent. These conditions lead to atactic polystyrene and a high degree of 1,4-addition of isoprene (75% cis-1,4; 20% trans-1,4; 5% 3,4 addition). The compositions of the diblock copolymers were calculated from the masses of the added monomers; the yield was 98%. The volume fraction of polyisoprene, f_{PI}, was estimated using the densities 0.969 and 0.83 g cm^{-3} for PS and PI at 413 K. The number–average molar mass, $\bar{M}_n$, has been calculated from the monomer/initiator ratio, which provides the most quantitative measure of $\overline{M}_n$. The sample, denoted SI58, is characterised by a volume fraction of PI, $f_{PI} = 0.58$, $\bar{M}_n = 21220$ g mol^{-1}, and a polydispersity index $\bar{M}_w/\bar{M}_n = 1.09$, which was determined by size exclusion chromatography. This method also provided a relative measure of the overall molecular weight and confirmed the absence of homopolymer. From $\bar{M}_n$, where the segment volume is defined as $v = \sqrt{v_{PI}v_{PS}} \cong 156$ Å^3 (413 K), we obtain a degree of polymerisation $N = 255$. Using a published expression [18] for the temperature dependence of χ:

$$\chi = 0.0118 + \frac{26.5}{T},$$

we thus determine that $\chi N = 18$ at the order–disorder transition (446 K). This places the sample in the intermediate segregation regime.

The entanglement molar mass for 1,4-polyisoprene $\bar{M}_e$ (298 K) = 5000 g mol^{-1}, whilst for polystyrene $\bar{M}_e$ (413 K) = 13000 g mol^{-1} [19]. Thus, in SI58 the polyisoprene block is unentangled whilst the polystyrene block is lightly entangled.

2.2. Rheology

Measurements of the dynamic shear moduli were performed using a Rheometrics RSA II rheometer. An oscillatory strain was applied to samples mounted in a shear sandwich configuration. Polymer films for rheology experiments were prepared by melting polymer between PTFE sheets in a vacuum oven.

Order–disorder phase transition temperatures were determined from isochronal temperature ramps, performed in the linear viscoelastic regime. The linear regime was identified from strain sweeps.

Stress relaxation experiments were conducted by applying a constant strain through out the experiment and recording the time dependent decay of stress. The strain amplitude varied from 0.1% up to 100%. The strain was increased in steps, and stress relaxation was allowed to continue for at least 250 s (which is sufficient for the modulus to reach a plateau) before measurements at the next strain. A second series of stress relaxation curves was then recorded, at the same strains as the first series of measurements. Due to alignment of the sample induced by large amplitude strains in the first sequence of strains, the stress relaxation curve differed in the second run. The relaxation curves were collected for 200 s in four time zones 2, 2, 6 and 190 s collecting 400 data points in each zone. Unless otherwise stated, all measurements were conducted in the ordered lamellar melt, at $T = 125$°C.

3. Results

The order–disorder transition (ODT) temperature for SI58 was determined from temperature ramp experiments at a frequency $\omega = 1$ rad s^{-1} ($\gamma = 1\%$ strain amplitude) starting at a temperature of 110°C with a heating rate of 2°C min^{-1} up to 200°C. The expected rapid drop of both G' and G'' at the ODT was apparent and this defined $T_{ODT} = (174 \pm 2)$°C. The ODT was also determined from discontinuities in small-angle X-ray scattering peak width and intensity to occur at $T_{ODT} = (172 \pm 2)$°C, in good agreement with the value from rheology.

Time-temperature superposed frequency sweep data (not shown) confirms an unoriented lamellar structure, since at low frequency both G' and G'' scale as $\omega^{1/2}$ [5,20]. This data also indicates a high frequency crossover at $\omega = 500$ rad s^{-1}, corresponding to a characteristic relaxation time of approximately 0.002 s.

Stress relaxation experiments provide information on the dynamics of relaxation processes. Experiments were conducted for several values of strain amplitude, from 0.3 to 100%, and the corresponding time dependent relaxation modulus, $G(t)$, was measured. Representative data are shown in Fig. 1, which also shows the results of the two measurements for a strain $\gamma = 70\%$. Despite the apparent significant difference in relaxation curves, the distribution of relaxation times is quite reproducible (vide infra). In the following, data from the first run on the unoriented sample are considered. The distribution of relaxation rates was obtained by fitting the relaxation modulus, through the equation:

$$G(t) = \int_{\lambda_{min}}^{\lambda_{max}} g(\lambda)\exp(-t\lambda)\mathrm{d}\lambda \quad (1)$$

where $g(\lambda)$ is a continuous function which was determined using the program CONTIN [21]. CONTIN can be used to fit the experimental data through Eq. (1), and provides a solution for $g(\lambda)$ as an inverse Laplace transform. Fig. 2 shows $g(\lambda)$ obtained for different imposed strains λ. Two

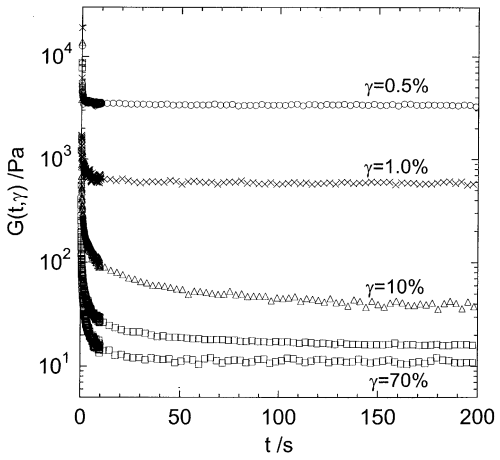

Fig. 1. Stress relaxation curve $G(t, \gamma)$ for four different strains (for $\gamma = 70\%$ two curves are shown to highlight differences in stress relaxation caused by sample alignment).

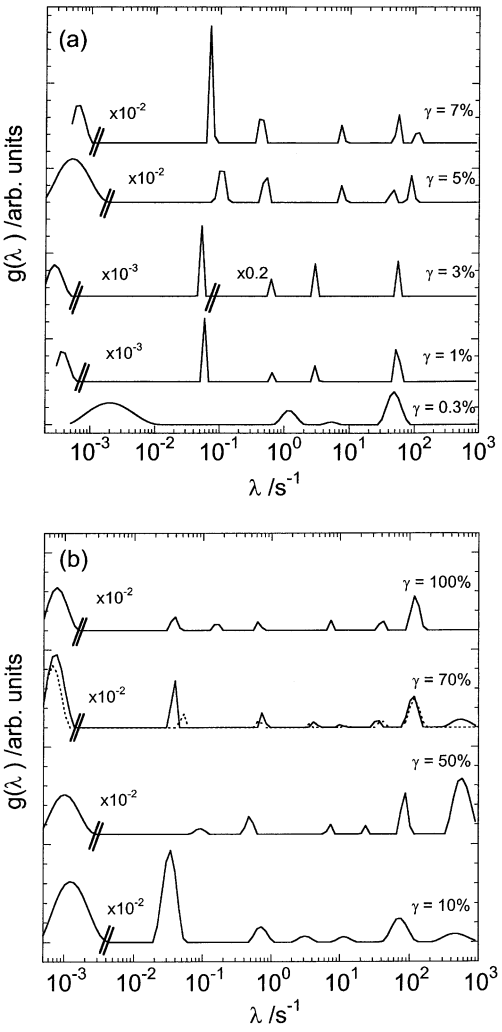

Fig. 2. Dependence of $g(\lambda)$ on the imposed strain γ, for (a) $\gamma = 0.3$, 1, 3, 5 and 7% and (b) $\gamma = 10$, 50, 70 and 100%. The curves have been arbitrarily shifted. For $\gamma = 70\%$ the dashed curve corresponds to the higher of the two stress relaxation curve for this strain shown in Fig. 1.

distributions are shown for $\gamma = 70\%$, corresponding to the two stress relaxation curves in Fig. 1. This highlights the reproducibility of the distribution of relaxation rates even when there are apparently significant differences in the input stress relaxation data. A representative fit to the experimental $G(t)$ through Eq. (1), is shown in Fig. 3 for $\gamma = 70\%$.

We determined $g(\lambda)$ only imposing a non-negativity constraint, but without constraining the number of peaks to a pre-determined value [21–23]. As shown in Fig. 2, CONTIN indicates that the number of peaks in $g(\gamma)$ varies as a function of γ, increasing from 4 for $\gamma = 0.3\%$ to 8 for $\gamma = 70\%$.

Each peak in $g(\lambda)$ is associated with a relaxation time of the system, τ_p, and can be used to approximate Eq. (1) via the expression:

$$G(t) = \sum_p g_p \exp(-t/\tau_p) \tag{2}$$

where $\lambda_p = 1/\tau_p$ corresponds to a maximum in $g(\lambda)$, and g_p is a constant. Fig. 4 shows the τ_p associated with the peaks in $g(\lambda)$ shown in Fig. 2. Fig. 3 compares, for $\gamma = 70\%$, the fit to the experimental $G(t)$ obtained with Eq. (2), (using the relaxation times plotted in Fig. 4) with the fitting provided by the CONTIN program, using the full distribution $g(\lambda)$ and not just the peaks.

The dynamics of block copolymer liquids (melts and solutions) is complex [1]. Previous dynamic light scattering results on symmetric [24–27] and asymmetric diblock co-polymer melts [28] have revealed multiple relaxation processes. The terminal relaxation time obtained from rheology experiments in the disordered state of a lamellar block copolymer was shown to be in quantitative agreement with the internal mode from dynamic light scattering experiments [27], which is a low amplitude process that is independent of wavenumber q. The internal mode arises from relative motion of the centres of mass of the two blocks [27,29]. A similar connection between a virtually q-independent mode from dynamic light scattering

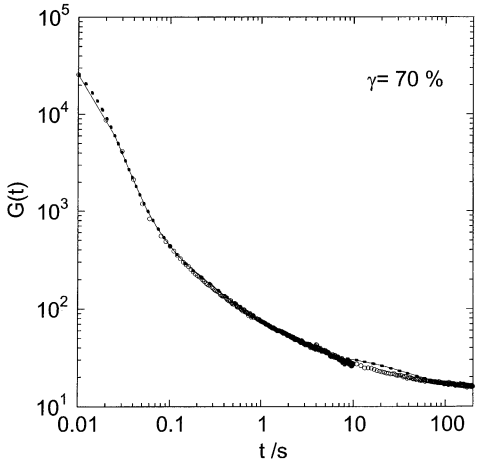

Fig. 3. Stress relaxation of the modulus $G(t)$ for $\gamma = 70\%$: solid line: fit using Eq. (1); dotted line: fit using Eq. (2).

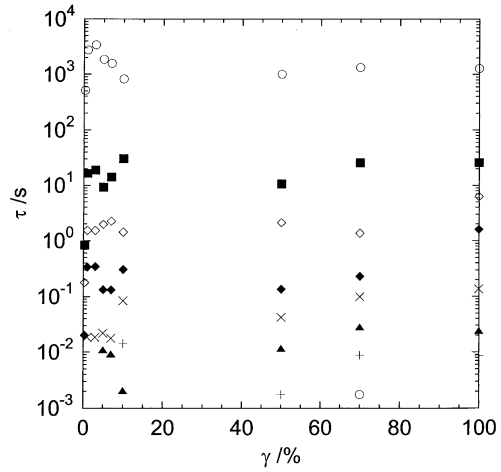

Fig. 4. Strain dependence of the relaxation times, τ_p, associated with the peaks in the corresponding $g(\lambda)$ shown in Fig. 2.

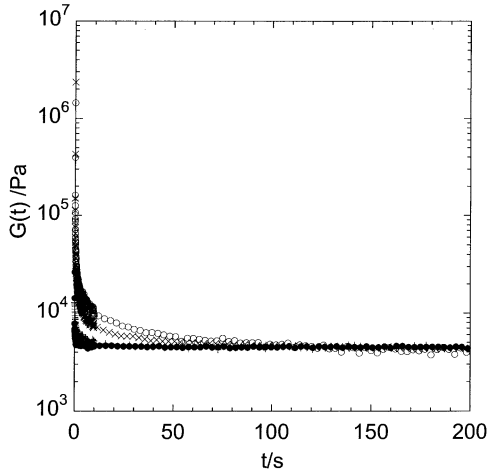

Fig. 5. Superposition of stress relaxation curves, $G(t)$, at long times. Four different strains are represented, corresponding to Fig.1: (●) $\gamma = 0.5\%$; (+) $\gamma = 1.0\%$; (○) $\gamma = 10\%$; (x) $\gamma = 70\%$.

and the terminal relaxation time obtained from rheology has been established for semidilute and concentrated polymer solutions [30]. In the following, the timescale of the relaxation processes obtained from our stress relaxation experiments is compared to non-diffusive slow modes observed via field gradient NMR and dynamic light scattering experiments on similar microphase-separated lamellar diblock copolymer melts. However, it is not possible to establish a connection between diffusive modes observed via other techniques and relaxation processes observed rheologically, because diffusive timescales vary as q^{-2}, whereas rheological timescales must be q independent. Thus the so-called 'cluster' and 'heterogeneity' modes, both of which have been identified as diffusive modes [1,26] via dynamic light scattering cannot be identified from rheology experiments.

The smallest timescale observed for all strains in Fig. 1 is $\tau_{fast} \sim 0.01$ s, and its magnitude can be compared to relaxation times obtained from field gradient NMR experiments on a symmetric polystyrene–polyisoprene diblock ($\bar{M}_n = 15700$, $T_{ODT} = 89°C$) both above and below the ODT [31]. This sample is somewhat more weakly segregated than our sample, but qualitative comparisons are possible. Below the ODT, Fleisher et al. identified a slow, diffusive, process with $t \sim 6$ s and a non-diffusive process with $\tau \sim 0.033$ s. The latter is quite close to τ_{fast} obtained for our sample. Papadakis and coworkers [26] presented results from a dynamic light scattering study of the melt of a symmetric polystyrene–polybutadiene diblock ($\bar{M}_n = 18300$ g mol^{-1}, $T_{ODT} = 130°C$) that is similar in chemistry, molecular weight and ODT to SI58. A 'heterogeneity' mode was observed with $\tau \sim 0.1$ s (at 135°C). They also observed an 'internal' mode, with $\tau \sim 5.7$ ms. This is comparable to τ_{fast} observed at low strains (Fig. 4).

We are not able to provide a physical interpretation of the intermediate relaxation timescales in Fig. 4. However, we do suggest an interpretation of the slowest relaxation process observed (τ_{slow}). It is strain dependent, decreasing by about a factor of three from low strains to a strain $\gamma = 100\%$ (Fig. 4). The strain dependence of this timescale, together with its slowness, suggest that this process is related to the relaxation of shear-induced orientation. Typical results from sheared block copolymer melts indeed confirm that the (partial) relaxation of shear-induced orientation of the microstructure occurs over a timescale of minutes or hours [32–38]. Furthermore, we expect that relaxation will be faster at higher strains, as indeed observed.

The relaxation modulus for a relaxation process in the non-linear regime can, in general, be factored into two parts, a time dependent component, $G(t)$, and a strain dependent damping function, $h(\gamma)$: [39]

$$G(t, \gamma) = G(t)h(\gamma) \tag{3}$$

At low strain $G(t, \gamma)$ is close to $G(t)$, within experimental uncertainty. By vertical shifting of $G(t, \gamma)$ with respect to the relaxation modulus for the lowest strain at large time scales it is possible to determine the damping function, $h(\gamma)$. The long-time superposition of modulus relaxation curves is illustrated in Fig. 5. The calculated $h(\gamma)$ from the superposition of the relaxation modulus are plotted against the strain in Fig. 6. Two different approaches to explain the strain dependence of the damping function are used here. First, we consider plastic flow for which the stress, σ, is independent of strain above the yield stress, and therefore $G(t, \gamma) = \sigma(t)/\gamma$ scales as γ^{-1} [40]. It follows that the damping function scales as γ^{-1} above the yield stress. The solid line in Fig. 5 shows a fit to $h(\gamma) = c\gamma^{-1}$, where c is a constant, and the agreement with the data indicates that plastic flow dominates at higher strain. However, deviations are apparent for small strains. To account for the crossover in $h(\gamma)$ at small strain, a more complicated damping function must be considered. We show in Fig. 6

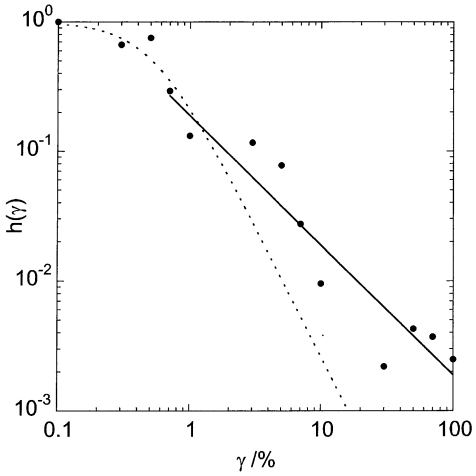

Fig. 6. The damping function $h(\gamma)$ obtained from the superposition of modulus relaxation data $G(t, \gamma) = G(t)h(\gamma)$. The solid line is a fit to $h(\gamma) = c\gamma^{-1}$, where c is an adjustable parameter, and the dotted represents a fit function obtained by Larson [41], $h(\gamma) = 1/(1 + \alpha\gamma^2/3)$, where α is the fit parameter.

a fit to the damping function obtained for shear flow in the Larson model: [41–43]

$$h(\gamma) = \frac{1}{1 + \alpha\gamma^2/3} \tag{4}$$

The Larson model starts from a constitutive equation that is a differential equation with time-strain separability. It contains has only one parameter, that describes the strain softening or hardening character of the material. The model has been shown to fit quite well a wide range of non-linear rheology data for homopolymer melts [40]. A fit to Eq. (4) is shown in Fig. 6. The equation agrees well with the experimental data at low strain but cannot take in to account the effects at higher strain, as expected since it is apparent that our block copolymer exhibits plastic flow at high strain. The parameter $\alpha = 1.1 \times 10^5$, indicating that the material is strongly strain softening [42], as indeed evident from the data in Fig. 1. If we allow the exponent of γ in Eq. (3) to vary from $n = 2$, an excellent fit is obtained with $\alpha = 4125$, $n = 1.25$ (data not shown).

4. Conclusions

The non-linear dynamic mechanical behaviour of a polystyrene–polyisoprene diblock copolymer forming a lamellar phase has been investigated, in particular the stress relaxation behaviour as a function of strain amplitude has been analysed using a regularized inverse Laplace transform method. This is the first report, to our knowledge, on the relaxation processes in microphase-separated block copolymers via analysis of the stress relaxation function. The results indicates a complex relaxation process, with multiple relaxation timescales. Despite the microphase separation in the structure, time-strain separability of the modulus is still possible as observed for many homopolymers in the melt and solution. In contrast to these latter systems, the damping function $h(\gamma)$ for the lamellar-forming block copolymer is consistent with a strongly strain softening system exhibiting plastic flow at large strains. The large decrease in modulus observed on increasing strains was also confirmed via strain sweeps at low frequencies (not shown), which also indicated pronounced strain-softening behaviour.

Acknowledgements

This work was conducted within the framework of the European Union Training and Mobility of Researchers network ‘Complex Architectures in Diblock Copolymer-Based Polymer Systems’.

References

[1] Hamley IW. The Physics of Block Copolymers. Oxford: Oxford University Press, 1998.
[2] Bates FS, Fredrickson GH. Physics Today 1999;52:32.
[3] Chung CI, Gale JC. J Polym Sci Polym Phys Ed 1976;14:1149.
[4] Gouinlock EV, Porter RS. Polym Eng Sci 1977;17:535.
[5] Rosedale JH, Bates FS. Macromolecules 1990;23:2329.
[6] Fredrickson GH, Bates FS. Annu Rev Mater Sci 1996;26:501.
[7] Watanabe H, Kotaka T, Hashimoto T, Shibayama M, Kawai H. J Rheol 1982;26:153.
[8] Watanabe H, Sato T, Osaki K, Yao M-L, Yamagishi A. Macromolecules 1997;30:5877.
[9] Hamley IW, Pople JA, Fairclough JPA, Ryan AJ, Booth C, Yang Y-W. Macromolecules 1998;31:3906.
[10] Daniel C, Hamley IW, van Dusschoten D, Wilhelm M, Mingvanish W. Rheol Acta 2000 in press.
[11] Honeker CC, Thomas EL. Chem Mater 1996;8:1702.
[12] Wiesner U. Macromol Chem Phys 1997;198:3319.
[13] Keller A, Pedemonte E, Willmouth FM. Nature 1970;225:538.
[14] Folkes MJ, Keller A. Polymer 1971;12:222.
[15] Odell JA, Keller A. Polym Eng Sci 1977;17:544.
[16] Ndoni S, Papadakis C, Bates FS, Almdal K. Rev Sci Instrum 1995;66:1090.
[17] Frielinghaus H, Hermsdorf N, Almdal K, Mortensen K, Hamley IW, Messé L, Corvazier L, Ryan AJ, van Dusschoten D, et al. Macromolecules (in press).
[18] Lin CC, Jonnalagadda SV, Kesani PK, Dai HJ, Balsara NP. Macromolecules 1994;27:7769.
[19] Fetters LJ, Lohse DJ, Colby RH. In: Mark JE, Physical Properties of Polymers Handbook. Woodbury, New York: American Institute of Physics, 1996. p. 335–40.
[20] Kawasaki K, Onuki A. Phys Rev A 1990;42:3664.
[21] Provencher SW. Comput Phys Comm 1982;27:229.
[22] Provencher SW. Makromol Chem 1979;180:201.
[23] Provencher SW. Comput Phys Comm 1982;27:213.
[24] Jian T, Anastasiadis SH, Semenov AN, Fytas G, Adachi K, Kotaka T. Macromolecules 1994;27:4762.
[25] Anastasiadis SH, Chrissopoulou K, Fytas G, Appel M, Fleischer G, Adachi K, Gallot Y. Acta Polym 1996;47:250.
[26] Papadakis CM, Brown W, Johnsen RM, Posselt D, Almdal K. J Chem Phys 1996;104:1611.
[27] Stepanek P, Lodge TP. Macromolecules 1996;29:1244.
[28] Papadakis CM, Almdal K, Mortensen K, Rittig F, Fleischer G, Stepanek P. Euro Phys J E 2000;1:275.

[29] Jian T, Semenov AN, Anastasiadis SH, Fytas G, Yeh F-J, Chu B, Vogt S, Wang F, Roovers JEL. J Chem Phys 1994;100:3286.
[30] Jian T, Vlassopoulos D, Fytas G, Pakula T, Brown W. Colloid Polym Sci 1996;274:1033.
[31] Fleischer G, Fujara F, Stühn B. Macromolecules 1993;26:2340.
[32] Hamley IW, Gehlsen MD, Khandpur AK, Koppi KA, Rosedale JH, Schulz MF, Bates FS, Almdal K, Mortensen K. J Phys France II 1994;4:2161.
[33] Koppi KA, Tirrell M, Bates FS, Almdal K, Mortensen K. J Rheol 1994;38:999.
[34] Zhang U, Wiesner U. J Chem Phys 1995;103:4784.
[35] Hajduk DA, Tepe T, Takenouchi H, Tirrell M, Bates FS, Almdal K, Mortensen K. J Chem Phys 1998;108:326.
[36] Chen Z-R, Kornfield JA, Smith SD, Grothaus JT, Satkowski MM. Science 1997;277:1248.
[37] Chen Z-R, Kornfield JA. Polymer 1998;39:4697.
[38] Vigild ME, Almdal K, Mortensen K, Hamley IW, Fairclough JPA, Ryan AJ. Macromolecules 1997;31:5702.
[39] Larson RG. The structure and rheology of complex fluids. New York: Oxford University Press, 1999.
[40] Macosko CW. Rheology. Principles, measurements and applications. New York: VCH, 1994.
[41] Larson RG. J Rheol 1984;28:545.
[42] Khan SA, Larson RG. J Rheol 1987;31:207.
[43] Khan SA, Prudhomme RK, Larson RG. Rheol Acta 1987;26:144.